

1. Fundamentals of Fluid Dynamics

1.1 Introduction

As pointed out in the Preface, the major thrust of this text is to extend our discussion of spectral methods from the simple model problems and single-domain methods described in the companion book, CHQZ2, to practical applications in fluid dynamics and to methods for complex domains. We refer the reader to Chap. 8 for a short introduction to spectral methods.

As preparation for the applications that are the focus of Chaps. 2–4, in this chapter we provide a survey of the fundamentals of fluid dynamics. We begin with some general background material on fluids on fluids, then concentrate on the basic equations of fluid dynamics (in Eulerian form). These equations are first stated in their full generality for compressible flow. Subsequent expositions include various special cases, especially those to which spectral methods have most commonly been applied. These special cases include Euler equations, incompressible Navier–Stokes equations, boundary-layer equations, and equations for both linear and nonlinear stability analysis. We also include some historical background on the various systems of equations that have been used over the years in the study of fluid dynamics.

The reader interested in detailed derivations and physical interpretations of these equations should consult standard references such as Courant and Friedrichs (1976), Howarth (1953), Liepmann and Roshko (2001), Landau and Lifshitz (1987), Serrin (1959a), Moore (1989), Batchelor (2000), Schlichting and Gersten (1999), and the various texts on more specialized topics cited below. (Most of these texts have been published in several editions. We have listed them here in the chronological order of their first editions but provide a reference to the most recent edition as of the publication of this text; we use this convention for ordering references throughout this book.)

1.2 Fluid Dynamics Background

Gases, such as air, and liquids, such as water, are both fluids. Before proceeding to the partial differential equations that describe the motion of such fluids, we provide the basis for the distinction between these two types of fluids and then summarize the relevant thermodynamic relationships.

1.2.1 Phases of Matter

The phases of matter may be broadly categorized into solids and fluids. Simply stated, solids resist deformation and retain a rigid shape; in particular, the stress is a function of the strain. Fluids do not resist deformation and take on the shape of its container owing to their inability to support shear stress in static equilibrium. More precisely, the stress is a function of the strain rate. The distinction between solids and fluids is not so simple and is based upon both the viscosity of the matter and the time scale of interest. The inorganic polymer-based toy known as Silly Putty™ in the U.S. (and Pongo™ in Italy), for instance, can be considered either as a solid or as a fluid, depending on the time period over which it is observed. Fluids include liquids, gases and plasmas. A liquid is a fluid with the property that it conforms to the shape of its container while retaining its constant volume independent of pressure. A gas is a compressible fluid that not only conforms to the shape of its container but also expands to occupy the full container. Plasma is ionized gas. The various phases of a substance are represented by a *phase diagram*, which marks the domains in pressure–temperature where each phase exists. Figure 1.1 illustrates the well-known phase diagram for water.

A rigorous mathematical description of the states of matter appears implausible. Goodstein (1975) states: “Precisely what do we mean by the term liquid? Asking what is a liquid is like asking what is life; we usually know it when we see it, but the existence of some doubtful cases makes it hard to define precisely.” In his book, Anderson (1963) asks: “(2) How does one describe a solid from a really fundamental point of view in which the atomic nuclei as well as electrons are treated truly quantum mechanically? (3) How and why does a solid hold itself together? I have never yet seen a satisfactory fully quantum mechanical description of a solid.” Phase diagrams would seem to require well-defined criteria, but there are always states at the boundaries of the so-called “phases” that cannot be precisely defined.

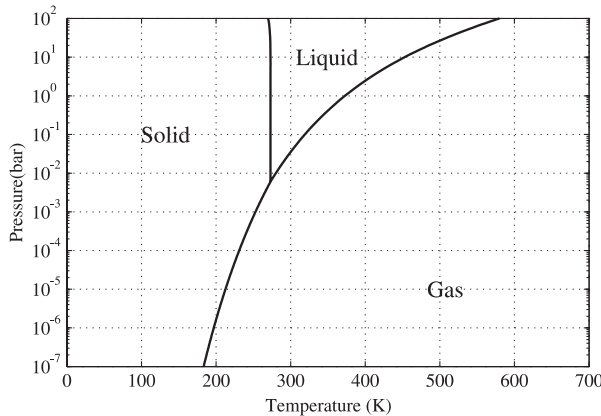


Fig. 1.1. Phase diagram for water

To be extremely precise, one should speak of “fluid-like” and “solid-like” behavior; their distinction depends upon the time and the length scales of interest. Glaciers and the Earth’s mantle flow are thus fluid-like if the time scale is appropriately large, while they can be considered as solids if the time scale is appropriately small. However, it is not merely a matter of the time scale. Even if the time scale is on the order of months and the length scale on the order of miles, the Earth’s mantle can be modeled as a solid, while if the length scale is the order of nanometers or less it may be appropriate to model it as a fluid. This suggests the need for appropriate nondimensional numbers. In rational mechanics, the nondimensional Deborah number (see Huilgol (1975)) is the ratio of a process time to an inherent relaxation time. The same lump of borosiloxane can be observed to flow as a fluid if the time scale is sufficiently large, to deform like an elastic solid, or to shatter like brittle glass.

Perhaps, the most accurate and lucid discussion of the distinction between solid-like and fluid-like behavior was given by Maxwell (1872): “What is required to alter the form of a soft solid is a sufficient force, and, this when applied produces its effect at once. In the case of viscous fluid it is time that is required, and if enough time is given, the very smallest force will produce a sensible effect, such as would require a very large force if suddenly applied. Thus a block of pitch may be so hard that you cannot make a dent in it by striking it with your knuckles; and yet it will in course of time, flatten itself by its own weight, and glide down hill like a stream of water.” Maxwell is clearly referring to the importance of time scales and to a material that seems to have two time scales. However, materials can have more than two time scales.

1.2.2 Thermodynamic Relationships

General Gases. A complete description of a single-phase, homogeneous fluid is available if, as a function of space and time, the velocity $\mathbf{u} = (u, v, w)^T$, any two thermodynamic variables, and an equation of state are known. (The superscript T denotes the transpose of a vector or matrix.). The basic thermodynamic variables of most interest in fluid dynamics are the density ρ (or specific volume $V = 1/\rho$), the pressure p , the temperature T , the specific internal energy e , the specific entropy s , and the specific enthalpy h . (A *specific* quantity is one per unit mass.) Of these state variables, only two are independent, and the others can be expressed as functions of the two independent variables. In the classical Gibbs axiomatic formulation, the equation of state is

$$e = e(V, s) , \quad (1.2.1)$$

and the variables *pressure* and *temperature* are defined by

$$p = -\frac{\partial e}{\partial V} \quad \text{and} \quad T = \frac{\partial e}{\partial s} , \quad (1.2.2)$$

respectively, where p and T are always positive. By forming the total differential of the relation $e = e(V, s)$, we obtain the fundamental thermodynamic relation

$$T ds = de + p dV . \quad (1.2.3)$$

This may be considered a corollary of the second law of thermodynamics, and it defines the *specific entropy*, denoted by s .

The (specific) *total energy* is defined as

$$E = e + \frac{1}{2}(\mathbf{u} \cdot \mathbf{u}) , \quad (1.2.4)$$

the (specific) *enthalpy* is defined as

$$h = e + p/\rho , \quad (1.2.5)$$

and the (specific) *total enthalpy* is defined as

$$H = h + \frac{1}{2}(\mathbf{u} \cdot \mathbf{u}) . \quad (1.2.6)$$

The various relations among p , V , T , e , and s are known as *equations of state*. Relations giving p as a function of ρ (or V) and s (or T) occur with the greatest frequency in the theory of fluids:

$$p = f_1(\rho, T) \quad \text{or} \quad p = f_2(V, s) \quad \text{or} \quad p = f_3(\rho, s) . \quad (1.2.7)$$

Such relations are usually referred to as *caloric equations of state*. A unit mass of fluid in thermodynamic equilibrium has two important heat capacities

$$C_v = T \left. \frac{\partial s}{\partial T} \right|_V \quad \text{and} \quad C_p = T \left. \frac{\partial s}{\partial T} \right|_p . \quad (1.2.8)$$

They are called, respectively, the *specific heat at constant volume* and the *specific heat at constant pressure*. Experimental observations support the assumption that both specific heats are always positive. Using (1.2.3) and the corresponding total differential of the enthalpy, one obtains

$$C_v = \left. \frac{\partial e}{\partial T} \right|_V \quad \text{and} \quad C_p = \left. \frac{\partial h}{\partial T} \right|_p . \quad (1.2.9)$$

From (1.2.3) and the first part of (1.2.9), we have

$$C_p - C_v = \left(p + \left. \frac{\partial e}{\partial V} \right|_T \right) \left. \frac{\partial V}{\partial T} \right|_p . \quad (1.2.10)$$

Differentiating (1.2.3) with respect to T and V , respectively, we have

$$\left. \frac{\partial s}{\partial T} \right|_V = \frac{1}{T} \left. \frac{\partial e}{\partial T} \right|_V , \quad \left. \frac{\partial s}{\partial V} \right|_T = \frac{1}{T} \left(p + \left. \frac{\partial e}{\partial V} \right|_T \right) . \quad (1.2.11)$$

Then, equating the derivative of the former with respect to V with the derivative of the latter with respect to T , we have

$$p + \left. \frac{\partial e}{\partial V} \right|_T = \left. \frac{\partial p}{\partial T} \right|_V . \quad (1.2.12)$$

Hence, using (1.2.12) in (1.2.10), we have for the difference between the specific heats:

$$C_p - C_v = -\frac{T}{\rho^2} \left. \frac{\partial p}{\partial T} \right|_\rho \left. \frac{\partial \rho}{\partial T} \right|_p . \quad (1.2.13)$$

(See Howarth (1953) for more details.)

Another important positive quantity is

$$c^2 = \left. \frac{\partial p}{\partial \rho} \right|_s , \quad (1.2.14)$$

where c is called the *sound speed*, which is the speed at which sound waves travel in the fluid (see Sect. 4.3).

Perfect Gases. The preceding equations are the general thermodynamic relationships. A number of special cases are of practical interest. A *thermally perfect gas* (also known as an *ideal gas*) is a fluid that obeys *Boyle's Law*, which is expressed by the equation of state

$$p = \rho \mathcal{R} T , \quad (1.2.15)$$

where the gas constant \mathcal{R} is the ratio of the universal gas constant to the effective molecular weight of the particular gas.

In many applications the fluid is assumed to be calorically perfect in addition to being thermally perfect. For a thermally perfect gas one can show that both the specific internal energy and the specific enthalpy are functions of temperature only:

$$de = C_v(T) dT \quad \text{and} \quad dh = C_p(T) dT . \quad (1.2.16)$$

A thermally perfect gas is called *calorically perfect* if the specific heats are independent of temperature:

$$e = C_v T \quad \text{and} \quad h = C_p T , \quad (1.2.17)$$

assuming of course that both e and h vanish if T vanishes. Equations (1.2.4) and (1.2.6) become, respectively,

$$E = C_v T + \frac{1}{2}(\mathbf{u} \cdot \mathbf{u}) \quad (1.2.18)$$

and

$$H = C_p T + \frac{1}{2}(\mathbf{u} \cdot \mathbf{u}) . \quad (1.2.19)$$

It can be proven that an ideal gas that is calorically perfect has the *polytropic equation of state*

$$p = f(\rho, s) = K\rho^\gamma, \quad (1.2.20)$$

where K depends on the entropy only and γ (called the *adiabatic exponent*) is the ratio of the specific heats, C_p/C_v . Its value lies in the interval $1 < \gamma < 5/3$ for most fluids, and it is usually assumed to be 1.4 for air at moderate temperatures ($< 800^\circ\text{K}$).

For a calorically perfect gas (1.2.14) becomes

$$c^2 = \frac{\gamma p}{\rho}, \quad (1.2.21)$$

and (1.2.13) reduces to

$$C_p - C_v = \mathcal{R}. \quad (1.2.22)$$

The latter equation leads to the relations

$$C_p = \frac{\gamma}{\gamma - 1}\mathcal{R} \quad \text{and} \quad C_v = \frac{1}{\gamma - 1}\mathcal{R}, \quad (1.2.23)$$

and the calorically perfect gas equation of state

$$p = \frac{\rho e}{\gamma - 1}. \quad (1.2.24)$$

Furthermore, we have that

$$\gamma = \frac{C_p}{C_v}. \quad (1.2.25)$$

1.2.3 Historical Perspective

Before commencing our summary of the basic equations of fluid dynamics, we provide a brief historical perspective on the evolution of the mathematical description of fluid motion. Navier (1827) must be credited with the first attempt at deriving the equations for homogeneous incompressible viscous fluids on the basis of considerations involving the action of intermolecular forces. Poisson (1831) derived the equations for compressible fluids from a similar molecular model. The first mathematical description of the motion of an “ideal” (inviscid and incompressible) fluid was, however, due to Euler (1755), who applied Newton’s second law of motion to a fluid moving under an internal force known as the pressure gradient. D’Alembert (1752) was the first to point out that this mathematical model leads to the eponymous paradox that a body at rest in a uniform stream of ideal fluid suffers no drag: “a singular paradox which I leave to geometricians to explain”. Although Navier’s (1827) intermolecular interaction model did include a viscous term, which was proportional to the Laplacian of the velocity field, he did not recognize the physical significance of viscosity and considered the viscosity

coefficient to be a function of molecular spacing. The continuum derivation of the Navier–Stokes equations is due to Saint-Venant (1843) and Stokes (1845). Saint-Venant published a derivation of the equations on a more physical basis that applied not only to the so-called laminar flows considered by Navier but also to turbulent flows. However, it was Stokes who, under the sole assumption that the stresses are linear functions of the strain rates, derived the equations in the form that is currently in use. Interesting details of the history of fluid dynamics can be found in Truesdell (1953), Darrigol (2002), and in the texts by Rouse and Ince (1963) and Grattan-Guinness (1990).

As noted above, Euler (1755) was the first to provide a mathematical description of the motion of inviscid fluids. The Euler equations are often used to simulate vortical flows such as those resulting from shocks or breakaway separations whose basic mechanisms are not dominated by viscous effects. The matched asymptotic expansion theories (van Dyke (1975), Moore (1989)) have established the relevance of the Euler solution as the first term of the outer expansion to be matched with the first term of the inner expansion, which describes the relatively thin boundary layer abutting the solid streamlined boundary. Thus, the Euler solution coupled with corrections from the boundary-layer equations are sometimes used as an alternative to solving the relatively expensive full Navier–Stokes equations.

Prototypes of the concept of a boundary layer associated with the no-slip condition on a solid body had existed since the derivation of the equations of motion of a viscous fluid (Stokes (1845), Rankine (1864), Froude (1872), Lorenz (1881)). However, it was Prandtl (1904) who first derived what are now known as the boundary-layer equations based on the dimensional argument that in the thin layer adjacent to a body in a stream, the viscous stress in the streamwise direction is much larger than the normal stress and is of the same order of magnitude as the streamwise inertial force. The formal mathematical basis for deriving the boundary-layer theory from the Navier–Stokes equations was achieved by Lagerstrom and associates (see van Dyke (1969)), who developed the singular perturbation theory or method of matched asymptotic expansions. Simply stated, this consists of constructing the so-called outer and inner expansions by iterating the Navier–Stokes equations between an outer inviscid solution (that does not satisfy the no-slip condition on the body) and an inner solution (that satisfies the no-slip condition on the body) and matching them in their overlapping region of validity. Tani (1977) provides an excellent historical perspective on boundary-layer theory.

1.3 Compressible Fluid Dynamics Equations

This section begins with the most general form of the fluid dynamics equations considered in this text, namely, the compressible Navier–Stokes equations. Then various special or limiting forms of the compressible equations

are presented. The following section focuses on the incompressible versions of these equations.

1.3.1 Compressible Navier–Stokes Equations

The constitutive equations are essential to the description of a viscous fluid. These are equations that relate the viscous stress tensor $\underline{\tau}$ at a given point $\mathbf{x} = (x, y, z)$ of the medium to the strain tensor $\underline{\mathbf{S}}$ at that point. The term *Stokesian fluid* is used for fluids that satisfy the conditions that the stress tensor (i) is a continuous function of the strain tensor (and independent of all other kinematic quantities), (ii) is spatially homogeneous, (iii) is spatially isotropic, and (iv) is equal to $-p\underline{\mathbf{I}}$ (where $\underline{\mathbf{I}}$ is the unit tensor and p is a scalar) if the strain vanishes. These imply (see, e.g., Serrin (1959a)), that the stress tensor is a linear combination of the identity matrix, the strain tensor, and the square of the strain tensor. *Classical fluids* are those for which the additional condition that the stress tensor is a linear function of the strain tensor is imposed. (The term Newtonian fluid is sometimes used for classical fluids, although this term is more properly applied to just the incompressible situation.) This yields the classical constitutive equation for the total stress tensor $\underline{\sigma}$:

$$\underline{\sigma} = -p\underline{\mathbf{I}} + \underline{\tau} , \quad (1.3.1)$$

with the viscous stress tensor

$$\underline{\tau} = 2\mu\underline{\mathbf{S}} + \lambda(\nabla \cdot \mathbf{u})\underline{\mathbf{I}} , \quad (1.3.2)$$

and the strain-rate tensor

$$\underline{\mathbf{S}} = \frac{1}{2}[\nabla\mathbf{u} + (\nabla\mathbf{u})^T] . \quad (1.3.3)$$

Here, μ and λ are called the *first* and *second coefficients of viscosity*, respectively. The first coefficient of viscosity μ is also called the *shear viscosity* and often simply the viscosity. The symbols $\nabla \cdot$ and ∇ denote the divergence and gradient operators, respectively, with respect to the spatial coordinate \mathbf{x} .

The *viscous dissipation function* Φ , which represents the work done by the viscous stresses on a particle, is defined as

$$\Phi = \underline{\tau} : \nabla\mathbf{u} , \quad (1.3.4)$$

with the colon denoting the contraction of the double-index tensors. The constraint that the dissipation function is always nonnegative requires that

$$\mu \geq 0 \quad \text{and} \quad \left(\lambda + \frac{2}{3}\mu \right) \geq 0 . \quad (1.3.5)$$

The expression $(\lambda + \frac{2}{3}\mu)$ is called the *bulk viscosity*. The limiting case corresponding to $\mu = \lambda = 0$ yields a simplified model, the Euler equations, discussed in Sect. 1.3.4.

When the effect of thermal conduction is significant, one uses the *Fourier law*

$$\mathbf{q} = -\kappa \nabla T \quad (1.3.6)$$

to express the *heat flux* \mathbf{q} as a function of the temperature gradient through the *thermal conductivity* κ .

The relationship between κ and μ is customarily written in terms of the *Prandtl number*, defined as

$$\text{Pr} = \frac{C_p \mu}{\kappa} . \quad (1.3.7)$$

This is the nondimensional ratio of the viscous diffusion to the thermal conductivity. The length scale for viscous diffusion is greater than or less than the length scale for thermal conductivity depending upon whether Pr is less than or greater than 1, respectively. In general, the Prandtl number is not constant, although the simplifying assumption of a constant Prandtl number is very common in applications.

The coefficients of viscosity and the thermal conductivity are dependent upon the thermodynamic variables, primarily the temperature. For gases, the shear viscosity is commonly taken from *Sutherland's formula*

$$\frac{\mu}{\mu_r} = \frac{T_r + S_1}{T + S_1} \left(\frac{T}{T_r} \right)^{3/2} , \quad (1.3.8)$$

where μ_r is the viscosity at the reference temperature T_r , S_1 is a constant, and the temperature T is given in degrees Kelvin. For air, $S_1 = 110.4^\circ\text{K}$, and for the reference values $T_r = 273.1^\circ\text{K}$ and $\mu_r = 1.716 \times 10^{-4}$ gm/cm-sec, (1.3.8) becomes

$$\mu = \frac{1.458 T^{3/2}}{T + 110.4} \times 10^{-5} \text{ gm/cm-sec} , \quad (1.3.9)$$

and the bulk viscosity is taken to be zero, yielding

$$\lambda = -\frac{2}{3}\mu . \quad (1.3.10)$$

The algebraic form of Sutherland's formula is based on molecular forces considerations (Sutherland (1893)), and the constants are determined by fitting experimental data for a given gas (Anon. (1949, 1953)); for air, it is quite accurate for temperatures between 100°K and 1890°K . Although empirical formulas for the thermal conductivity are also available, κ is often just taken to be proportional to μ , i. e., the Prandtl number Pr is taken to be strictly constant in (1.3.7). For example, $\text{Pr} = 0.7$ is usually used for air.

The *Navier-Stokes equations* are a differential form of the three conservation laws that govern the motion in time t of classical fluids. The conservation laws are first expressed in integral form as the appropriate conservation statement for any arbitrary volume that moves with the fluid, accounting for

any relevant surface effects. The partial differential equations then follow under suitable continuity and differentiability conditions. The *equation of mass conservation*, known as the continuity equation, is

$$\frac{\partial \rho}{\partial t} + \nabla \cdot (\rho \mathbf{u}) = 0 . \quad (1.3.11)$$

The *equation for momentum conservation* is

$$\frac{\partial(\rho \mathbf{u})}{\partial t} + \nabla \cdot (\rho \mathbf{u} \mathbf{u}^T) + \nabla p = \nabla \cdot \underline{\boldsymbol{\tau}} , \quad (1.3.12)$$

and the *equation for total energy conservation* is

$$\frac{\partial(\rho E)}{\partial t} + \nabla \cdot (\rho E \mathbf{u}) + \nabla \cdot (p \mathbf{u}) = -\nabla \cdot \mathbf{q} + \nabla \cdot (\underline{\boldsymbol{\tau}} \mathbf{u}) . \quad (1.3.13)$$

(In (1.3.12) the divergence of a tensor appears. The symbol $\nabla \cdot \underline{\boldsymbol{\tau}}$ indicates the vector whose components are $(\nabla \cdot \underline{\boldsymbol{\tau}})_i = \sum_j \frac{\partial \tau_{ij}}{\partial x_j}$.) The momentum conservation statement that leads to (1.3.12) utilizes Newton's second law via the Cauchy principle that allows one to express the surface forces in terms of the total stress (volumetric forces have been neglected). The Navier–Stokes equations (1.3.11)–(1.3.13) must be supplemented with an equation of state, e. g., (1.2.15) for ideal gases or (1.2.24) for calorically perfect gases.

When volumetric forces \mathbf{f} need to be taken into account, the momentum and total energy conservation laws become balance laws, whereas the mass conservation equation holds unchanged. In this more general case the Navier–Stokes equations read

$$\frac{\partial \rho}{\partial t} + \nabla \cdot (\rho \mathbf{u}) = 0 , \quad (1.3.14)$$

$$\frac{\partial(\rho \mathbf{u})}{\partial t} + \nabla \cdot (\rho \mathbf{u} \mathbf{u}^T) + \nabla p = \nabla \cdot \underline{\boldsymbol{\tau}} + \mathbf{f} , \quad (1.3.15)$$

$$\frac{\partial(\rho E)}{\partial t} + \nabla \cdot (\rho E \mathbf{u}) + \nabla \cdot (p \mathbf{u}) = -\nabla \cdot \mathbf{q} + \nabla \cdot (\underline{\boldsymbol{\tau}} \mathbf{u}) + \mathbf{f} \cdot \mathbf{u} . \quad (1.3.16)$$

Alternative forms of the energy equation in terms of specific (internal) energy e , entropy s , temperature T , and pressure p , are

$$\rho \left(\frac{\partial e}{\partial t} + \mathbf{u} \cdot \nabla e \right) + p \nabla \cdot \mathbf{u} = -\nabla \cdot \mathbf{q} + \Phi , \quad (1.3.17)$$

$$\rho T \left(\frac{\partial s}{\partial t} + \mathbf{u} \cdot \nabla s \right) = -\nabla \cdot \mathbf{q} + \Phi , \quad (1.3.18)$$

$$\rho \frac{\partial(C_v T)}{\partial t} + \rho \mathbf{u} \cdot \nabla(C_v T) + p \nabla \cdot \mathbf{u} = -\nabla \cdot \mathbf{q} + \Phi , \quad (1.3.19)$$

$$\frac{\partial p}{\partial t} + \mathbf{u} \cdot \nabla p + \gamma p \nabla \cdot \mathbf{u} = (\gamma - 1)[- \nabla \cdot \mathbf{q} + \Phi] . \quad (1.3.20)$$

Equations (1.3.11)–(1.3.18) apply even for non-ideal gases. The equation for the temperature (1.3.19), however, is specialized to thermally perfect gases, while the equation for the pressure (1.3.20) is restricted even further to calorically perfect gases.

The alternatives (1.3.17)–(1.3.20) hold even in the presence of volumetric forces, which appear explicitly in (1.3.16) but in none of these alternative equations. For the most part, in the remainder of this chapter our discussion presumes that volumetric forces are neglected, although elsewhere in this text they are quite often included.

Numerical computations of compressible Navier–Stokes problems are most commonly based on the conservation forms, (1.3.11)–(1.3.13). The alternative forms for the energy equation, (1.3.19)–(1.3.20), are used occasionally for stability analysis and for computations of compressible flows that have no discontinuities.

The previous equations hold at any point \mathbf{x} of the region Ω occupied by the fluid at a given time. If the boundary $\partial\Omega$ of Ω consists of a solid, stationary wall, then the boundary conditions on $\partial\Omega$ are no-slip for velocity,

$$\mathbf{u} = \mathbf{0} ,$$

and some appropriate temperature condition, commonly either constant temperature,

$$T = T_{\text{wall}} ,$$

or adiabatic conditions,

$$\kappa \frac{\partial T}{\partial n} = \kappa \nabla T \cdot \mathbf{n} = 0 ,$$

where \mathbf{n} is the outward (with respect to Ω) unit vector normal to the boundary.

The Navier–Stokes equations are an incompletely parabolic system (Belov and Yanenko (1971), Strikwerda (1976)); the absence of a diffusion term in the continuity equation prevents them from being fully parabolic. Consequently, there are only four boundary conditions on solid walls, but there needs to be a fifth boundary condition at open boundaries at those points for which $\mathbf{u} \cdot \mathbf{n} < 0$. The appropriate choice of mathematical boundary conditions on inflow and outflow boundaries is rather subtle. As discussed by Gustafsson and Sundstrom (1978) and Oliger and Sundstrom (1978), one desires not just that the problem be mathematically well-posed, but also that there be no nonphysical boundary layers near the inflow and outflow boundaries. For example, consider a flow in a two-dimensional channel with solid boundaries on the top and the bottom, an inflow boundary on the left and an outflow boundary on the right. There will be viscous boundary layers next to the two walls, but there should not be any boundary layers at the inflow and outflow boundaries other than those near the walls. This will be achieved if the imposed boundary conditions yield a well-posed problem in the inviscid limit. See the above references for further details.

The mathematical analysis of the compressible Navier–Stokes equations can be found in Serrin (1959b), Matsumura and Nishida (1979), Valli (1983), P.-L. Lions (1998), and Hoff (2002, 2006).

1.3.2 Nondimensionalization

The mathematical statement of a particular flow problem involves specification of geometric, flow and fluid parameters—some characteristic (or reference) length L_{ref} (such as the distance between two enclosing boundaries as in channel flow, or the maximum linear dimension of a solid body), characteristic length velocity U_{ref} (such as the free-stream velocity), characteristic temperature T_{ref} , pressure p_{ref} and density ρ_{ref} (based, for example, on free-stream conditions and related by $p_{\text{ref}} = \rho_{\text{ref}} \mathcal{R} T_{\text{ref}}$), viscosity μ_{ref} and conductivity κ_{ref} .

Let us introduce nondimensional quantities identified with superscript $*$:

$$\begin{aligned} \mathbf{x}^* &= \frac{\mathbf{x}}{L_{\text{ref}}}, & t^* &= \frac{U_{\text{ref}} t}{L_{\text{ref}}}, & \mathbf{u}^* &= \frac{\mathbf{u}}{U_{\text{ref}}}, & p^* &= \frac{p}{p_{\text{ref}}}, & \rho^* &= \frac{\rho}{\rho_{\text{ref}}}, \\ E^* &= \frac{E}{U_{\text{ref}}^2}, & \mu^* &= \frac{\mu}{\mu_{\text{ref}}}, & \lambda^* &= \frac{\lambda}{\mu_{\text{ref}}}, & \kappa^* &= \frac{\kappa}{\kappa_{\text{ref}}}, \end{aligned} \quad (1.3.21)$$

and let ∇^* denote differentiation with respect to \mathbf{x}^* .

The key dimensionless parameters that arise are the reference Mach number, the *Reynolds number* and the reference Prandtl number parameters:

$$M_{\text{ref}} = \sqrt{\frac{\rho_{\text{ref}} U_{\text{ref}}^2}{\gamma p_{\text{ref}}}}, \quad \text{Re} = \frac{\rho_{\text{ref}} U_{\text{ref}} L_{\text{ref}}}{\mu_{\text{ref}}}, \quad \text{Pr}_{\text{ref}} = \frac{\mu_{\text{ref}} C_p}{\kappa_{\text{ref}}}. \quad (1.3.22)$$

(The Mach number and the Prandtl number also have the more local meanings given in (1.3.46) and (1.3.7), respectively. As we only consider flows with constant Prandtl number in this text, we henceforth drop the subscript $_{\text{ref}}$ on the Prandtl number in the nondimensional equations. We do, however, retain this subscript to ensure the distinction between the reference Mach number used for nondimensionalization and the local Mach number of the flow.)

In terms of these nondimensional coordinates, variables and parameters, the compressible Navier–Stokes equations (1.3.11)–(1.3.13) for a calorically perfect gas are

$$\frac{\partial \rho^*}{\partial t^*} + \nabla^* \cdot (\rho^* \mathbf{u}^*) = 0, \quad (1.3.23)$$

$$\frac{\partial (\rho^* \mathbf{u}^*)}{\partial t^*} + \nabla^* \cdot (\rho^* \mathbf{u}^* \mathbf{u}^{*T}) + \frac{1}{\gamma M_{\text{ref}}^2} \nabla^* p^* = \frac{1}{\text{Re}} \nabla^* \cdot \boldsymbol{\tau}^*, \quad (1.3.24)$$

$$\begin{aligned} & \frac{\partial (\rho^* E^*)}{\partial t^*} + \nabla^* \cdot (\rho^* E^* \mathbf{u}^*) + (\gamma - 1) \nabla^* \cdot (p^* \mathbf{u}^*) \\ &= \frac{\gamma}{\text{PrRe}} \nabla^* \cdot (\kappa^* \nabla^* T^*) + \gamma(\gamma - 1) \frac{M_{\text{ref}}^2}{\text{Re}} \nabla^* \cdot (\boldsymbol{\tau}^* \mathbf{u}^*); \end{aligned} \quad (1.3.25)$$

the nondimensional (ideal gas) equation of state is

$$p^* = \rho^* T^* , \quad (1.3.26)$$

and the nondimensional viscous stress tensor and strain tensor are, respectively,

$$\underline{\tau}^* = 2\mu^* \underline{\mathbf{S}}^* + \lambda^* (\nabla^* \cdot \mathbf{u}^*) \underline{\mathbf{I}} , \quad (1.3.27)$$

$$\underline{\mathbf{S}}^* = \frac{1}{2} [\nabla^* \mathbf{u}^* + (\nabla^* \mathbf{u}^*)^T] . \quad (1.3.28)$$

Various limiting cases of these equations have important applications. The resulting simplified systems of equations are discussed later in this section and in the following section.

1.3.3 Navier–Stokes Equations with Turbulence Models

The Navier–Stokes equations were derived from first principles. They are appropriate for use in numerical computations for which all relevant spatial and temporal scales are resolved. This is usually feasible for laminar flow, but rarely feasible for turbulent flow. See CHQZ2, Sect. 1.3 for a detailed discussion of temporal and spatial scales in turbulent flow. In particular, we recall that for isotropic turbulence the range of spatial scales increases as $\text{Re}^{3/4}$ in each direction, and that the range of temporal scales grows as $\sqrt{\text{Re}}$. For sufficiently small Reynolds numbers Re , all the scales can be resolved. The term *direct numerical simulation* (DNS) is often used to describe computations of time-dependent flows in which all the scales are resolved.

For most fluid dynamical engineering applications turbulence effects are important and DNS of such turbulent flows is impractical. Hence, the Navier–Stokes equations are often augmented with turbulence models. *Reynolds-averaged Navier–Stokes* (RANS) turbulence models are the norm in engineering. (See the references in Sect. 1.4.2 for discussions of RANS models for incompressible flow and Wilcox (1993) for some particulars for compressible flow.) *Large-eddy simulation* (LES) models emerged in the 1970s as a research tool for turbulence flow physics research and began to make a limited impact in engineering applications in the 1990s. Various hybrid RANS/LES approaches have been developed. These use RANS models in part of the flow and LES models in other parts. One example is the *detached-eddy simulation* (DES) approach (see Spalart (2000)) that uses RANS models in attached boundary layers and LES models in regions of separated flow.

Sagaut (2006) provides extensive coverage of LES formulations and models, albeit only for incompressible flow. Pope (2000) discusses LES for compressible (and reacting) flows. Gatski, Hussaini and Lumley (1996) provide an introduction to DNS, LES and RANS modeling of turbulent flows. Spalart (2000) reviews RANS, LES and DES models.

The LES and RANS equations are derived from the Navier–Stokes equations by an averaging procedure. This involves filtering out the chaotic, fluctuating, small-scale, high-frequency motions, and modeling their effect on the slowly varying, smooth eddies for the dependent variables in the new governing equations. For example, for homogeneous flows a filter function $\bar{\mathbf{u}}(\mathbf{x}, t)$ is often defined as

$$\bar{\mathbf{u}}(\mathbf{x}, t) = \int \int G(\mathbf{x} - \mathbf{x}', t - t', \mathbf{x}, t) \mathbf{u}(\mathbf{x}', t') d\mathbf{x}' dt', \quad (1.3.29)$$

where G is the weight or filter function in space and/or time. This has compact support (i. e., it vanishes outside a finite domain within which it assumes finite values) and satisfies

$$\int \int G(\mathbf{x} - \mathbf{x}', t - t', \mathbf{x}, t) d\mathbf{x}' dt' = 1. \quad (1.3.30)$$

The filtering procedure needs to be properly adapted when one approaches the boundary; see, e. g., Sagaut (2006) for a discussion of appropriate LES filters near boundaries.

The key step in the derivation of the LES or RANS equations is averaging over small scales by the aforementioned procedures applied to the Navier–Stokes equations. (The RANS equations are often derived using an ensemble or temporal average; their equivalence to spatial averaging through some sort of ergodic hypothesis is not proven, but generally assumed.) What distinguishes LES from RANS is the definition of the small scales. LES assumes the small scales to be smaller than the mesh size Δ , and RANS assumes them to be smaller than the largest eddy scale L .

To illustrate the basic concept and the resulting closure problem, consider the simple scalar equation

$$\frac{\partial u}{\partial t} + \frac{\partial}{\partial x}(uu) = 0, \quad (1.3.31)$$

and write

$$u = \bar{u} + u', \quad (1.3.32)$$

where \bar{u} is the filtered (or averaged) value of u , and u' is the fluctuating component. Applying the filtering operator (1.3.29) to (1.3.32) and assuming that G is chosen so that the filtering and differentiation operators commute, we have

$$\frac{\partial \bar{u}}{\partial t} + \frac{\partial}{\partial x}(\overline{uu}) = 0. \quad (1.3.33)$$

After moving the nonlinear term to the right-hand side and adding $\partial(\bar{u}\bar{u})/\partial x$ to both sides, we obtain

$$\frac{\partial \bar{u}}{\partial t} + \frac{\partial}{\partial x}(\bar{u}\bar{u}) = -\frac{\partial}{\partial x}(\overline{uu} - \bar{u}\bar{u}). \quad (1.3.34)$$

If the filter function G satisfies

$$G^2 = G \quad (1.3.35)$$

(such a filter is called a *Reynolds operator*), then

$$\overline{\bar{u}} = \bar{u} \ , \quad \overline{u'} = 0 \ , \quad (1.3.36)$$

and $(\overline{uu} - \bar{u}\bar{u}) = \overline{u'u'}$. The filter functions used for RANS are time averages or ensemble averages; these RANS filters are typically Reynolds operators. The term $\overline{u'u'}$ is the *subgrid-scale stress* (also called the *residual stress*) for this simple equation (1.3.31), and it must be modeled. The filters used in LES usually do not satisfy (1.3.35). (An exception that does satisfy (1.3.36) is the sharp cutoff filter in Fourier space.)

We focus here on the LES equations since spectral methods have been used far more for LES computations than for RANS or DES computations. Indeed, classical spectral methods figured prominently in many of the early LES computations in the 1970s and 1980s. (As in CHQZ2, we distinguish between spectral methods in single domains, termed classical spectral methods, and the multidomain spectral methods appropriate for applications in complex geometries.) Applications of RANS (and DES) methods are almost invariably for problems in complex geometries, for which classical spectral methods are inappropriate. However, use of multidomain spectral methods for RANS of smooth flows in complex geometries would only be productive if the error due to the RANS modeling were less important than the discretization error. In most RANS applications for complex flows, the uncertainty due to the turbulence model overwhelms the uncertainty due to discretization error.

For compressible LES, as for RANS, the averaged equations simplify if a Favre (density-weighted) average, denoted by a tilda, is used for some of the variables. For example, the Favre-averaged velocity is given by

$$\tilde{\mathbf{u}} = \frac{\overline{\rho \mathbf{u}}}{\bar{\rho}} \ . \quad (1.3.37)$$

The LES equations for compressible flow that result from Favre averaging are the continuity equation

$$\frac{\partial \bar{\rho}}{\partial t} + \nabla \cdot (\bar{\rho} \tilde{\mathbf{u}}) = 0 \ , \quad (1.3.38)$$

the momentum equation (the meaning of the superscript c will be given below)

$$\frac{\partial (\bar{\rho} \tilde{\mathbf{u}})}{\partial t} + \nabla \cdot (\bar{\rho} \tilde{\mathbf{u}} \tilde{\mathbf{u}}^T) + \nabla \bar{p} - \nabla \cdot \underline{\boldsymbol{\tau}}^c = \nabla \cdot (\underline{\boldsymbol{\tau}} - \underline{\boldsymbol{\tau}}^c) \ , \quad (1.3.39)$$

the energy equation

$$\begin{aligned} & \frac{\partial(\bar{\rho}\tilde{E})}{\partial t} + \nabla \cdot (\bar{\rho}\tilde{\mathbf{u}}\tilde{E}) + \nabla \cdot (\bar{p}\tilde{\mathbf{u}}) + \nabla \cdot \mathbf{q}^c - \nabla \cdot (\boldsymbol{\tau}^c\tilde{\mathbf{u}}) \\ &= -\nabla \cdot \left[\bar{\rho}(\widetilde{\mathbf{u}E} - \tilde{\mathbf{u}}\tilde{E}) \right] - \nabla \cdot (\bar{\mathbf{q}} - \mathbf{q}^c) - \nabla \cdot (\bar{p}\tilde{\mathbf{u}} - \bar{p}\tilde{\mathbf{u}}) + \nabla \cdot (\boldsymbol{\tau}\tilde{\mathbf{u}} - \boldsymbol{\tau}^c\tilde{\mathbf{u}}) , \end{aligned} \quad (1.3.40)$$

and the (ideal gas) equation of state

$$\bar{p} = \bar{\rho} \mathcal{R} \tilde{T} . \quad (1.3.41)$$

Note that the total energy in (1.3.40) is given by

$$\bar{\rho}\tilde{E} = \frac{\bar{p}}{\gamma - 1} + \frac{1}{2} \bar{\rho} \widetilde{\mathbf{u} \cdot \mathbf{u}} . \quad (1.3.42)$$

The resolved kinetic energy is computed from the trace of modeled subgrid-scale stresses, assuming that, unlike the typical situation for incompressible flows, the full subgrid-scale tensor (and not just its anisotropic part—see (1.4.11)) is modeled.

The energy equation (1.3.40) is only one of several possible formulations found in the literature. Alternate formulations include equations for the pressure, internal energy, enthalpy, and a modified total energy $\widehat{\rho E} = \bar{\rho}(\tilde{e} + \frac{1}{2}\tilde{\mathbf{u}} \cdot \tilde{\mathbf{u}})$.

Terms on the right-hand side of (1.3.39)–(1.3.40) must be modeled. The full descriptions of the compressible LES models are quite complicated. We refer the reader to Yoshizawa (1986) and to Speziale, Erlebacher, Zang and Hussaini (1988) for some early models, and to Pope (2000) for a more thorough coverage. A representative complete LES model for the simpler case of incompressible flow is provided below in Sect. 1.4.2.

A superscript c refers to nonlinear functions in which each variable is replaced by its resolved value (simple average or Favre average as the case may be) to permit an approximate evaluation. In particular, the spatial average of the viscous stresses are

$$\bar{\tau}_{ij} = \overline{2\mu S_{ij}} + \overline{\lambda \delta_{ij} S_{kk}} ,$$

while a computable form of the viscous stress tensor is

$$\tau_{ij}^c = 2\mu^c \tilde{S}_{ij} + \lambda^c \delta_{ij} \tilde{S}_{kk} .$$

The viscosities are in general functions of temperature, and their computable forms are defined by $\mu^c = \mu(\tilde{T})$ and $\lambda^c = \lambda(\tilde{T})$. Note that the temperature appears naturally as a Favre-averaged quantity. In the energy equation, the heat fluxes are

$$\bar{\mathbf{q}} = -\overline{\kappa \nabla T} , \quad \mathbf{q}^c = -\kappa^c \nabla \tilde{T} ,$$

with a resolved-scale, temperature-dependent conductivity $\kappa^c = \kappa(\tilde{T})$.

1.3.4 Compressible Euler Equations

As noted in Sect. 1.3.2, various limiting cases of the nondimensionalized Navier–Stokes equations are of interest. If one lets $\text{Re} \rightarrow \infty$, i.e., $\mu \rightarrow 0$, in (1.3.23)–(1.3.25), then all the terms on the right-hand sides vanish, and one obtains the *Euler equations*. In dimensional form these are

$$\frac{\partial \rho}{\partial t} + \nabla \cdot (\rho \mathbf{u}) = 0, \quad (1.3.43)$$

$$\frac{\partial(\rho \mathbf{u})}{\partial t} + \nabla \cdot (\rho \mathbf{u} \mathbf{u}^T) + \nabla p = \mathbf{0}, \quad (1.3.44)$$

$$\frac{\partial(\rho E)}{\partial t} + \nabla \cdot (\rho \mathbf{u} E) + \nabla \cdot (p \mathbf{u}) = 0, \quad (1.3.45)$$

supplemented with an equation of state. (These equations coincide with the Navier–Stokes equations (1.3.11)–(1.3.13) if the right-hand side terms are disregarded.) Quite apart from their engineering use in obtaining acceptable physical solutions, the Euler equations are frequently used in the analysis and development of numerical algorithms that are eventually applied to the Navier–Stokes equations.

This system is hyperbolic. It admits weak or discontinuous solutions (Courant and Friedrichs (1976), Lax (1973)). The order of the Euler equations is reduced by one compared with the full Navier–Stokes equations, leading to the loss of the velocity no-slip boundary condition and the boundary condition on the temperature (or other thermodynamic variable). The boundary conditions at stationary solid walls are no-flux:

$$\mathbf{u} \cdot \mathbf{n} = 0.$$

The conditions at inflow or outflow boundaries are dependent upon the characteristic directions there. Appropriate boundary conditions are discussed in Sect. 4.3.

The flow is called *subsonic* at a point \mathbf{x} and a time t if $|\mathbf{u}| < c$ and *supersonic* if $|\mathbf{u}| > c$. The (local) *Mach number* M is given by

$$M = |\mathbf{u}|/c. \quad (1.3.46)$$

In order for the flow to change from a supersonic state to a subsonic one, it must (except in rare circumstances) pass through a shock wave. Here the flow variables are discontinuous and the differential equations themselves do not apply, although the more basic integral conservation laws still hold.

1.3.5 Compressible Potential Equation

Experience has shown that rather accurate predictions can be made of a number of compressible flows of practical importance under the assumption that

the flow is irrotational, i. e., that the vorticity is zero (Lighthill (1989), Holst and Ballhaus (1979)). In this case, the velocity is derivable from a *velocity potential* ϕ , i. e.,

$$\mathbf{u} = \nabla\phi, \quad (1.3.47)$$

and (1.3.43) becomes the *compressible potential equation*

$$\frac{\partial\rho}{\partial t} + \nabla \cdot (\rho\nabla\phi) = 0, \quad (1.3.48)$$

where ρ is related to $\nabla\phi$ by the isentropic relation

$$\rho = \rho_0 \left[1 + \frac{\gamma - 1}{2} \frac{|\nabla\phi|^2}{c^2} \right]^{1/(1-\gamma)}, \quad (1.3.49)$$

in which ρ_0 is the stagnation density, i. e., the density at a point at which the velocity is zero (a stagnation point). The momentum equation (1.3.44) is automatically satisfied. For steady flow, we have simply

$$\nabla \cdot (\rho\nabla\phi) = 0. \quad (1.3.50)$$

The compressible potential equation is often referred to as the *full potential equation* to distinguish it from related but more severe approximations, such as the transonic small disturbance equation. (It is worth recalling that the transonic small disturbance equation was the setting for the type-dependent (elliptic/hyperbolic) difference scheme of Murman and Cole (1971), which was the breakthrough that ignited the intense developments in CFD for aerospace applications in the ensuing decades.)

Despite its seemingly restrictive assumption, the full potential equation has been a popular design tool in industry. As an irrotational flow is isentropic (the Crocco theorem—see, for example, Liepmann and Roshko (2001)), it is but consistent to replace a shock with a singular surface, across which all flow quantities are discontinuous except entropy. Since, as shown for example in Moore (1989), the entropy jump across a shock is proportional to the third power of the shock strength (measured by the jump in Mach number), the potential flow approximation has been found particularly useful in the formulation of transonic flow problems where the shock Mach number is less than 1.3. The full potential solution can be coupled with the boundary-layer solution to incorporate viscous effects. The relatively low computational requirements (such as low storage per cell) of the potential model (Flores et al. (1985)) and its innate preclusion of spurious entropy generation at stagnation points (often afflicting Euler and Navier–Stokes algorithms) makes it an attractive alternative for treating flows past complex geometries of industrial interest on highly dense grids. However, it must be pointed out that although the full potential equation may provide accurate fixed-point solutions in valid regimes, it may not accurately predict trends such as the lift-versus-slope curve (Salas and Gumbert (1985)).

The desire for efficient numerical solutions of (1.3.50) for use in aircraft design motivated considerable progress in computational fluid dynamics in the late 1970s and early 1980s; see, e. g., Jameson (1978) and Glowinski (1984).

1.3.6 Compressible Boundary-Layer Equations

Prandtl (1904) introduced the concept of a *boundary layer*—a thin layer adjacent to solid walls to which the effects of viscosity are often confined. The so-called *boundary-layer equations* are the companion inner equations to the (outer) Euler equations. These inner equations are obtained by a special limit process. For a two-dimensional flow, let the coordinate system (x^*, y^*) be such that the x^* -coordinate is along the boundary of the solid body in the direction of the free stream, and y^* is normal to the boundary. Introducing the scaled normal coordinate and normal velocity,

$$\bar{y}^* = \frac{y^*}{\sqrt{\text{Re}}} , \quad \bar{v}^* = \frac{v^*}{\sqrt{\text{Re}}} ,$$

into (1.3.23)–(1.3.25) (see (1.5.14) for a particular choice of reference quantities) and letting $\text{Re} \rightarrow \infty$, one obtains the compressible boundary-layer equations, which in nondimensional form are

$$\frac{\partial \rho^*}{\partial t^*} + \frac{\partial(\rho^* u^*)}{\partial x^*} + \frac{\partial(\rho^* \bar{v}^*)}{\partial \bar{y}^*} = 0 , \quad (1.3.51)$$

$$\frac{\partial(\rho^* u^*)}{\partial t^*} + \frac{\partial(\rho^* u^* u^*)}{\partial x^*} + \frac{\partial(\rho^* u^* \bar{v}^*)}{\partial \bar{y}^*} + \frac{\partial p^*}{\partial x^*} = \frac{\partial}{\partial \bar{y}^*} \left(\mu^* \frac{\partial u^*}{\partial \bar{y}^*} \right) , \quad (1.3.52)$$

$$\begin{aligned} & \frac{\partial(\rho^* E^*)}{\partial t^*} + \frac{\partial(\rho^* u^* E^*)}{\partial x^*} + \frac{\partial(\rho^* \bar{v}^* E^*)}{\partial \bar{y}^*} + (\gamma - 1) \frac{\partial(\rho^* u^*)}{\partial x^*} + (\gamma - 1) \frac{\partial(\rho^* \bar{v}^*)}{\partial \bar{y}^*} \\ &= \frac{\gamma}{\text{Pr}} \frac{\partial}{\partial \bar{y}^*} \left(\kappa^* \frac{\partial T^*}{\partial \bar{y}^*} \right) + \gamma(\gamma - 1) \text{M}_{\text{ref}}^2 \left(\frac{\partial u^*}{\partial \bar{y}^*} \right)^2 . \end{aligned} \quad (1.3.53)$$

The wall-normal momentum equation reduces to $\partial p^* / \partial \bar{y}^* = 0$, which means that the pressure is constant across the boundary layer.

The customary version of the compressible boundary-layer equations for steady, two-dimensional flow is, in dimensional form,

$$\frac{\partial(\rho u)}{\partial x} + \frac{\partial(\rho v)}{\partial y} = 0 , \quad (1.3.54)$$

$$\rho u \frac{\partial u}{\partial x} + \rho v \frac{\partial u}{\partial y} = - \frac{\partial p}{\partial x} + \frac{\partial}{\partial y} \left(\mu \frac{\partial u}{\partial y} \right) , \quad (1.3.55)$$

$$\rho C_p u \frac{\partial T}{\partial x} + \rho C_p v \frac{\partial T}{\partial y} = u \frac{\partial p}{\partial x} + \frac{\partial}{\partial y} \left(\kappa \frac{\partial T}{\partial y} \right) + \mu \left(\frac{\partial u}{\partial y} \right)^2 , \quad (1.3.56)$$

where the total energy E has been replaced with the temperature T . These are supplemented by an equation of state. The boundary conditions are (for fixed wall temperature)

$$\begin{aligned} u = v = 0, \quad T = T_w & \quad \text{at } y = 0, \\ u = u_\infty, \quad T = T_\infty & \quad \text{at } y = \infty, \end{aligned} \quad (1.3.57)$$

plus appropriate inflow conditions at some $x = x_{\text{inflow}}$. The quantities u_∞ and T_∞ , as well as the (y -independent) pressure (all potentially functions of x) come from the outer solution. Some alternative wall temperature conditions are an adiabatic wall or a specified wall heat flux.

An important measure of the size of the boundary layer for flows past a solid body is the *displacement thickness* δ^* , defined (in the case of flow past a flat plate) by

$$\delta^* = \int_0^\infty \left(1 - \frac{\rho u}{\rho_\infty u_\infty} \right) dy. \quad (1.3.58)$$

It measures the deflection of the incident streamlines in the direction normal to the wall. A related measure is the *boundary-layer thickness* δ , commonly defined as the distance from the wall at which the velocity parallel to the wall has reached 99.5% (or sometimes 99.9%) of its free-stream value. In practice, this is a less precise measure than the displacement thickness.

1.3.7 Compressible Stokes Limit

In the limit $\text{Re} \rightarrow 0$, the viscous forces and the pressure forces balance each other. Hence, the appropriate scaling of pressure is

$$p^+ = \left(\frac{L_{\text{ref}}}{U_{\text{ref}} \mu_{\text{ref}}} \right) p = \left(\frac{\text{Re}}{\gamma M_{\text{ref}}^2} \right) p^*. \quad (1.3.59)$$

Introducing this new pressure variable into (1.3.23)–(1.3.25) and taking $\text{Re} \rightarrow 0$, one obtains the compressible Stokes equations

$$\frac{\partial \rho^*}{\partial t^*} + \nabla^* \cdot (\rho^* \mathbf{u}^*) = 0, \quad (1.3.60)$$

$$\nabla^* p^+ = \nabla^* \cdot \boldsymbol{\tau}^*, \quad (1.3.61)$$

$$0 = \frac{1}{\text{Pr}} \nabla \cdot (\kappa^* \nabla T^*) + \gamma(\gamma - 1) M_{\text{ref}}^2 \nabla^* \cdot (\boldsymbol{\tau}^* \mathbf{u}^*), \quad (1.3.62)$$

usually accompanied by the calorically perfect gas equation of state

$$\rho^* e^* = 1, \quad (1.3.63)$$

with e having the same scaling as E in (1.3.21).

1.3.8 Low Mach Number Compressible Limit

In the limit $M_{\text{ref}} \rightarrow 0$, the pressure term becomes singular in (1.3.24), thereby implying that the nondimensionalization of pressure with respect to the reference value in (1.3.21) is inappropriate. An appropriate nondimensionalized pressure for this limiting case is

$$\tilde{p} = \frac{p}{\rho_{\text{ref}} U_{\text{ref}}^2} = \frac{p^*}{\gamma M_{\text{ref}}^2}, \quad (1.3.64)$$

as pressure plays a dynamic role rather than a thermodynamic one.

Introducing this re-scaled pressure into (1.3.11)–(1.3.13), and then letting $M_{\text{ref}} \rightarrow 0$ yields the nondimensional compressible flow equations at zero Mach number:

$$\frac{\partial \rho^*}{\partial t^*} + \nabla^* \cdot (\rho^* \mathbf{u}^*) = 0, \quad (1.3.65)$$

$$\frac{\partial(\rho^* \mathbf{u}^*)}{\partial t^*} + \nabla^* \cdot (\rho^* \mathbf{u}^* \mathbf{u}^{*T}) + \nabla^* \tilde{p} = \frac{1}{\text{Re}} \nabla^* \cdot \boldsymbol{\tau}^*, \quad (1.3.66)$$

$$\frac{\partial(\rho^* E^*)}{\partial t^*} + \nabla^* \cdot (\rho^* \mathbf{u}^* E^*) = \frac{1}{\text{PrRe}} \nabla^* \cdot (\kappa^* \nabla^* T^*). \quad (1.3.67)$$

1.4 Incompressible Fluid Dynamics Equations

The equations described in the preceding section all have special forms in the incompressible limit. There are several different formulations of the incompressible Navier–Stokes equations. The most commonly used ones are the primitive variable (velocity and pressure), streamfunction-vorticity, and vorticity-velocity formulations. The primitive-variable formulation has been the one most extensively employed in large-scale three-dimensional calculations using spectral methods.

1.4.1 Incompressible Navier–Stokes Equations

The incompressible Navier–Stokes equations in primitive variable form can be derived from the low Mach number compressible limit if the additional assumption is made that the value of the nondimensional internal energy at the solid wall is $e_w^* = 1$. Then the equation of internal energy and the equation of state are identically satisfied by $\rho^* = 1$ and $e^* = 1$, and the above equations reduce to the incompressible flow equations. Thus a viscous fluid may be considered incompressible if the heat due to viscous dissipation and conduction is negligible, and the pressure variation causes negligible changes in internal energy or enthalpy.

In dimensional form the incompressible Navier–Stokes equations in a domain Ω are usually written as

$$\frac{\partial \mathbf{u}}{\partial t} + \mathbf{u} \cdot \nabla \mathbf{u} = -\nabla p + \frac{1}{2} \nabla \cdot [\nu (\nabla \mathbf{u} + \nabla \mathbf{u}^T)] + \mathbf{f}, \quad (1.4.1)$$

$$\nabla \cdot \mathbf{u} = 0, \quad (1.4.2)$$

where \mathbf{u} is the velocity vector, p is the pressure (divided by ρ), $\nu = \mu/\rho$ is the *kinematic viscosity*, \mathbf{f} are the volumetric forces (divided by ρ), and ρ is constant (and taken to be unity). Although for constant ν the viscous term in (1.4.1) can be written as just $\nu \Delta \mathbf{u}$ (where Δ is the Laplacian operator), we use the present form because of its greater generality. Equation (1.4.1) is the momentum equation and (1.4.2) is the continuity constraint. The equations above are in nonconservation form, unlike those in, say, (1.3.12) and (1.3.11). Observe that, due to (1.4.2), $\mathbf{u} \cdot \nabla \mathbf{u} = \nabla \cdot (\mathbf{u}\mathbf{u}^T)$. (This identity is generally lost at the discrete level.)

One would also include the limiting form of the energy equation if there were a temperature-dependent body force in the momentum equation or if the viscosity depended upon the temperature. The former situation includes the important case of Rayleigh–Bénard flow, for which (1.4.1) includes a buoyancy force linear in temperature, and the limiting form of the energy equation is an advection-diffusion equation for the temperature. However, since our analyses and examples in this text do not include Rayleigh–Bénard flow, we stick with the simpler set of equations above.

The pressure in the incompressible Navier–Stokes equations is not a thermodynamic variable satisfying an equation of state. Rather, it is an implicit dynamic variable that adjusts itself instantaneously in a time-dependent flow to satisfy the incompressibility, or divergence-free, condition. From the mathematical point of view, it may be considered as a Lagrange multiplier that ensures the kinematical constraint of incompressibility (i. e., solenoidity of the velocity field). Hence, no initial or boundary conditions are required for the pressure. Various results on the existence and uniqueness of solutions to the Navier–Stokes equations are furnished in the treatises on the mathematical analysis of these equations (J.-L. Lions (1969), Ladyženskaya (1969), Temam (2001), Kreiss and Lorentz (1989), Chorin and Marsden (1993), Foias, Manley, Rosa and Temam (2001), Galdi (1994a, 1994b), P-L. Lions (1996), Majda and Bertozzi (2002)).

1.4.2 Incompressible Navier–Stokes Equations with Turbulence Models

The LES equations for compressible flow were given in (1.3.38)–(1.3.40). Their incompressible version in the absence of volumetric forces is

$$\frac{\partial \bar{\mathbf{u}}}{\partial t} + \nabla \cdot (\bar{\mathbf{u}}\bar{\mathbf{u}}^T) + \nabla \bar{p} - \nabla \cdot \bar{\boldsymbol{\tau}} = -\nabla \cdot (\overline{\mathbf{u}\mathbf{u}^T} - \bar{\mathbf{u}}\bar{\mathbf{u}}^T), \quad (1.4.3)$$

$$\nabla \cdot \bar{\mathbf{u}} = 0, \quad (1.4.4)$$

with the viscous stress given by

$$\bar{\boldsymbol{\tau}} = -2\nu\bar{\mathbf{S}} ,$$

where the strain tensor $\bar{\mathbf{S}}$ is given in (1.3.3), the overbar denotes a filtering operation described by (1.3.30), and the viscosity has been assumed to be constant. Since the density is constant, the Favre averaging (1.3.37) reduces to the filtering operation (1.3.30).

The term on the right-hand-side of the momentum equation is the negative of the divergence of the total subgrid-scale stress

$$\tau_{ij}^{\text{SGS}} = \overline{\mathbf{u}\mathbf{u}^T} - \bar{\mathbf{u}}\bar{\mathbf{u}}^T , \quad (1.4.5)$$

and it requires a model. The remaining terms are all directly computable in terms of the average velocity and pressure, which are the dependent variables of the computation.

The Leonard (1974) decomposition of the subgrid-scale stress reads

$$\tau_{ij}^{\text{SGS}} = L_{ij} + C_{ij} + R_{ij} , \quad (1.4.6)$$

where

$$L_{ij} = (\overline{u_i u_j} - \bar{u}_i \bar{u}_j) , \quad (1.4.7)$$

$$C_{ij} = (\overline{u'_i u'_j} + \bar{u}_i \bar{u}'_j) , \quad (1.4.8)$$

$$R_{ij} = \overline{u'_i u'_j} , \quad (1.4.9)$$

are, respectively, the *Leonard stress*, the *cross stress* and the *Reynolds stress*. The Leonard and cross stresses vanish for Reynolds filters.

Many models for the Reynolds subgrid-scale stress are based on the simple *Smagorinsky model* (1963), which assumes that (i) the subgrid-scale fluctuations are isotropic and homogeneous, (ii) there is a Kolmogorov inertial range, $E(k) = C_K \epsilon^{2/3} k^{-5/3}$, and (iii) the mean dissipation rate $\epsilon = 2\nu\bar{\Delta} \int_0^{1/\bar{\Delta}} k^2 E(k) dk$. In the preceding expressions, k is the spatial wavenumber, $E(k)$ is the energy density, C_K is the Kolmogoroff constant and $\bar{\Delta}$ is the filter width; see, e. g., Hinze (1975) for a discussion of isotropic turbulence and the Kolmogoroff theory. The above assumptions lead to the choice of *eddy viscosity* as

$$\nu_t = (C_s \bar{\Delta})^2 \bar{S} \quad \text{with} \quad \bar{S} = \sqrt{2 \sum_{i,j=1}^3 \bar{S}_{ij} \bar{S}_{ij}} , \quad (1.4.10)$$

where $C_s^2 = (1/\pi^2)(1/(3C_K))^{3/2}$. The resulting Smagorinsky subgrid-scale model for the Reynolds stress is

$$\tau_{ij}^{\text{Smag}} = R_{ij} - \frac{1}{3} \delta_{ij} \sum_{k=1}^3 R_{kk} = -2\nu_t \bar{S}_{ij} , \quad (1.4.11)$$

with ν_t given by (1.4.10). Typically,

$$\bar{\Delta} = 2(\Delta x \Delta y \Delta z)^{1/3}, \quad (1.4.12)$$

with Δx , Δy and Δz the computational grid spacings in the three coordinate directions. The Smagorinsky constant is usually taken to be $C_s \approx 0.1$. (We caution the reader that several different conventions are used for this model; one will often not see a factor of 2 inside the square root in (1.4.10), and sometimes the Smagorinsky constant C_s is not squared.) Note that only the anisotropic part of the Reynolds stress is modeled. The isotropic part

$$\frac{1}{3} \delta_{ij} \sum_{k=1}^3 R_{kk}$$

can be absorbed into the pressure for incompressible flow (but not, of course, for compressible flow).

One improvement to this model that is often employed is the *dynamic Smagorinsky model*, which was proposed by Germano, Piomelli, Moin and Cabot (1991) and refined by Lilly (1992). This uses filters with two different widths to make the “constant” C_s depend upon time and usually also upon space. In addition to the *grid filter* on the scale $\bar{\Delta}$, one also employs a larger *test filter* on the scale $\hat{\Delta}$ (usually $\hat{\Delta} = 2\bar{\Delta}$). One then defines the so-called resolved turbulent stresses $\underline{\tau}^{\text{SGS,resolved}}$ and the subtest stresses $\underline{\tau}^{\text{SGS,subtest}}$, given by

$$\tau_{ij}^{\text{SGS,resolved}} = \widehat{\bar{u}_i \bar{u}_j} - \hat{u}_i \hat{u}_j, \quad \tau_{ij}^{\text{SGS,subtest}} = \widehat{\bar{u}_i \bar{u}_j} - \hat{u}_i \hat{u}_j. \quad (1.4.13)$$

Then, the modeling assumption

$$\begin{aligned} \tau_{ij}^{\text{SGS}} - \frac{1}{3} \delta_{ij} \sum_{k=1}^3 \tau_{kk}^{\text{SGS}} &= -2C_s \alpha_{ij}, \\ \tau_{ij}^{\text{SGS,subtest}} - \frac{1}{3} \delta_{ij} \sum_{k=1}^3 \tau_{kk}^{\text{SGS,subtest}} &= -2C_d \beta_{ij}, \end{aligned} \quad (1.4.14)$$

for some tensors $\underline{\alpha}$ and $\underline{\beta}$ is made. There are several choices for these tensors. One simple choice is

$$\alpha_{ij} = \hat{\Delta}^2 |\hat{\mathbf{S}}| \hat{S}_{ij}, \quad \beta_{ij} = \bar{\Delta}^2 |\bar{\mathbf{S}}| \bar{S}_{ij}. \quad (1.4.15)$$

Upon substitution of (1.4.14) into the *Germano identity* (Germano (1992)),

$$\tau_{ij}^{\text{SGS,resolved}} = \tau_{ij}^{\text{SGS,subtest}} - \hat{\tau}_{ij}^{\text{SGS}}, \quad (1.4.16)$$

and invocation of a least-squares minimization process, the dynamic Smagorinsky “constant” C_d is then computed from

$$C_d = -\frac{1}{2} \frac{\langle \sum_{i,j=1}^3 \tau_{ij}^{\text{SGS,resolved}} \gamma_{ij} \rangle}{\langle \sum_{i,j=1}^3 \gamma_{ij} \gamma_{ij} \rangle}, \quad (1.4.17)$$

where $\gamma_{ij} = \beta_{ij} - \hat{\alpha}_{ij}$, and $\langle \cdot \rangle$ represents an appropriate spatial averaging process. For example, in the case of homogeneous turbulence this would be a full three-dimensional spatial average, whereas for more complex flows, the spatial averaging would be more localized. All the quantities in (1.4.17) depend either directly upon the dependent variables in the LES computation, i. e., the β_{ij} , or can be computed by application of the test filter to the dependent variables, i. e., $\tau_{ij}^{\text{SGS,resolved}}$ and α_{ij} . (See Germano et al. (1991), Lilly (1992), Piomelli (2004), or Sagaut (2006) for more details and refinements.)

Alternative approaches to turbulence modeling based on the use of separate equations for the large and small scales, with the modeling confined to terms in the equations for the small scales, have been taken by Temam and coworkers (see, e. g., Dubois, Jauberteau and Temam (1998)) with the so-called *nonlinear Galerkin* method, and by Hughes and coworkers (see, e. g., the review paper by Hughes, Scovazzi and Franca (2004)) with the so-called *variational multiscale* method. They differ in the models used for the unresolved terms. These models are intrinsically connected to the underlying discretization and cannot be directly described solely in terms of a PDE system, as can the models already described. We defer further description to Sect. 3.3.5, where discretization approaches are discussed.

We refer the reader to the review by Lesieur and Metais (1996) and the text by Sagaut (2006) for thorough discussions of the subtle issues and the various subgrid-scale models that have been utilized in large-eddy simulation of incompressible flows. Some mathematical aspects of LES are discussed in Berselli, Iliescu and Layton (2006). RANS models for incompressible flow are very well-developed. As spectral methods have rarely been applied to RANS, we simply refer to Speziale (1991), Wilcox (1993), Chen and Jaw (1998) and Bernard and Wallace (2002) as some standard references on the subject.

1.4.3 Vorticity–Streamfunction Equations

One of the most interesting characteristics of a flow is its vorticity. This is denoted by ω and is given by

$$\omega = \nabla \times \mathbf{u}. \quad (1.4.18)$$

It represents (half) the local rotation rate of the fluid. A dynamical equation for the vorticity is derived by taking the curl of (1.4.1), which for the constant viscosity, unforced case yields

$$\frac{\partial \omega}{\partial t} + \mathbf{u} \cdot \nabla \omega = \omega \cdot \nabla \mathbf{u} + \nu \Delta \omega. \quad (1.4.19)$$

This is an advection-diffusion equation with the additional term $\boldsymbol{\omega} \cdot \nabla \mathbf{u}$. This term represents the effects of vortex stretching. It is identically zero for two-dimensional flows and is responsible for many of the interesting aspects of three-dimensional flows.

The vorticity can be combined with the streamfunction ψ to yield a concise description of two-dimensional flows. By setting $\mathbf{u} = (u, v, 0)^T$, a streamfunction ψ is defined by the relations

$$u = \frac{\partial \psi}{\partial y}, \quad v = -\frac{\partial \psi}{\partial x}; \quad (1.4.20)$$

the existence of such a function is guaranteed by the solenoidal property of \mathbf{u} . Taking the curl of the velocity and setting $\boldsymbol{\omega} = (0, 0, \omega)^T$, we obtain

$$\Delta \psi = -\omega. \quad (1.4.21)$$

Equation (1.4.19) reduces to

$$\frac{\partial \omega}{\partial t} + \frac{\partial \psi}{\partial y} \frac{\partial \omega}{\partial x} - \frac{\partial \psi}{\partial x} \frac{\partial \omega}{\partial y} = \nu \Delta \omega. \quad (1.4.22)$$

The flow is parallel to curves of constant ψ —the streamlines. In the case of steady, rigid walls, the boundary conditions that accompany (1.4.21)–(1.4.22) are

$$\psi = 0, \quad \frac{\partial \psi}{\partial n} = 0, \quad (1.4.23)$$

where $(\partial \psi / \partial n)$ represents the partial derivative of ψ in the direction normal to the wall.

Equations (1.4.21)–(1.4.23) provide a complete description of a two-dimensional incompressible flow; the velocity is then recovered through (1.4.20). Note that the pressure is not needed. The subtlety of the streamfunction-vorticity formulation is that there are no physical boundary conditions on the vorticity, but two boundary conditions on the streamfunction.

The elimination of the vorticity leads to the pure streamfunction formulation

$$\frac{\partial}{\partial t}(\Delta \psi) + \frac{\partial \psi}{\partial y} \frac{\partial}{\partial x}(\Delta \psi) - \frac{\partial \psi}{\partial x} \frac{\partial}{\partial y}(\Delta \psi) = \nu \Delta^2 \psi. \quad (1.4.24)$$

The extension of these approaches to three-dimensional flows requires the introduction of a second streamfunction or the use of a vector potential. The appropriate equations for the former can be found in Murdock (1986) and those for the latter in Brosa and Grossman (2002).

1.4.4 Vorticity–Velocity Equations

Another approach to eliminating the pressure from the incompressible Navier–Stokes equations is to take the curl of the momentum equation. There are

several versions of the resulting vorticity-velocity equations (see, e. g., Trujillo and Karniadakis (1999)). An example, for constant viscosity, is given by

$$\frac{\partial \boldsymbol{\omega}}{\partial t} + \nabla \times (\boldsymbol{\omega} \times \mathbf{u}) = -\nu \nabla \times (\nabla \times \boldsymbol{\omega}) , \quad (1.4.25)$$

$$\Delta \mathbf{u} = -\nabla \times \boldsymbol{\omega} , \quad (1.4.26)$$

$$\nabla \cdot \mathbf{u} = 0 . \quad (1.4.27)$$

The initial and boundary conditions on the velocity must be supplemented with initial and boundary conditions on the vorticity. The former are usually derived from the curl of the initial velocity field, and the latter from the boundary values of the curl of the instantaneous velocity field.

Although the vorticity-velocity equations have six dependent variables instead of the four associated with the primitive variable formulations, there are some circumstances in which they present computational advantages. One simple example will be given in Sect. 3.4.1.

1.4.5 Incompressible Boundary-Layer Equations

Prandtl's boundary-layer approximation for incompressible flow yields the following lowest-order terms from (1.4.1) and (1.4.2):

$$u \frac{\partial u}{\partial x} + v \frac{\partial u}{\partial y} = -\frac{\partial p}{\partial x} + \nu \frac{\partial^2 u}{\partial y^2} , \quad (1.4.28)$$

$$\frac{\partial u}{\partial x} + \frac{\partial v}{\partial y} = 0 . \quad (1.4.29)$$

The boundary conditions are

$$\begin{aligned} u = v = 0 & \quad \text{at } y = 0 , \\ u = u_\infty & \quad \text{at } y = \infty , \end{aligned} \quad (1.4.30)$$

plus appropriate inflow conditions at some $x = x_\infty$ and the prescribed pressure gradient.

1.5 Linear Stability of Parallel Flows

Even though a particular time-dependent Navier–Stokes problem may admit an equilibrium solution, i. e., a solution of the steady Navier–Stokes equations, that equilibrium solution may not be physically attainable due to instability (in time or in space) of the flow to small disturbances. The question of whether a given equilibrium solution is stable or unstable is crucial to many applications.

Rayleigh (1880) initiated the development of incompressible, inviscid linear stability theory. A subsequent series of papers by Rayleigh (see Mack

(1984)) established the theory of linear instability of inviscid flows as an eigenvalue problem governed by a second-order ordinary differential equation for the amplitude of the disturbance, with the disturbance wavenumber and frequency as parameters; this equation is now known as the Rayleigh equation. Apart from its importance in its own right, it provided two of the four independent fundamental solutions of the asymptotic viscous theory developed later. A key result of the inviscid linear theory is that the existence of an inflection point in the equilibrium velocity profile of the flow, i. e., a point at which the curvature of the profile vanishes, is a necessary condition for instability. In other words, there can be neither unstable nor neutral waves in a flow characterized by a velocity profile without an inflection point. As viscosity is supposed to have a diffusive effect, this led to the disturbing conclusion that flows with convex velocity profiles (e. g., boundary-layer flows) are stable, which conflicts with observations.

Although the formative ideas on the destabilizing influence of viscosity were propounded in Taylor (1915) and independently by Prandtl (1921), the genesis of an asymptotic viscous theory is ascribed to Tollmien (1929) and Schlichting (1933) (see Schlichting and Gersten (1999), Mack (1984)). The viscosity-induced instability waves of unidirectional flows are usually called Tollmien–Schlichting waves. The asymptotic viscous theory was put on a rather rigorous mathematical basis by Lin (1945) and Wasow (1948). Despite all these mathematical developments, the asymptotic viscous theory only attracted serious attention in the fluid mechanics community after its validation by the landmark experiments of Schubauer and Skramstad (1947), where unstable waves just like those predicted by the theory were observed. Since the early 1960s, the asymptotic theories have been supplanted in practical applications by numerical solutions of the governing differential equations. See (Drazin and Reid (2004), Schmid and Henningson (2001), and Criminale, Jackson and Joslin (2003) for a thorough coverage of fluid dynamics stability.

In applications to flows past such vehicles as aircraft and submarines, a limitation of the linear theory is that although it can predict the critical value of the Reynolds number at which instability commences, it can predict neither where the laminar boundary layer will start to break down (transition onset) nor where the laminar-turbulent transition will be complete. However, linear stability theory has underpinned a semi-empirical criterion, known as the e^N method, for predicting the onset of transition in low disturbance environments. This was proposed by Smith and Gamberoni (1956) and Van Ingen (1956) and is still widely used in engineering applications (Malik (1989)). This method states that transition occurs roughly when linear theory predicts that an initial disturbance will have grown by a factor of e^N . The optimum choice of N is application-dependent, but it is usually in the range $N = 9\text{--}11$.

In this section we describe the mathematical formulation of the linear stability problem for *parallel flows*, which are flows for which the mean flow

is a function of a single coordinate direction, and the mean velocity is perpendicular to that direction.

1.5.1 Incompressible Linear Stability

Let \mathbf{u}_0 and p_0 denote the velocity and pressure of an equilibrium solution (hereafter termed “mean flow”) to the constant-viscosity, unforced, incompressible Navier–Stokes equations. Then write $\mathbf{u} = \mathbf{u}_0 + \mathbf{u}'$ and $p = p_0 + p'$, where \mathbf{u}' and p' are perturbations to the mean flow. If \mathbf{u}' and p' are presumed small, and quadratic terms are neglected, then (1.4.1)–(1.4.2) become

$$\frac{\partial \mathbf{u}}{\partial t} + \mathbf{u}_0 \cdot \nabla \mathbf{u} + \mathbf{u} \cdot \nabla \mathbf{u}_0 = -\nabla p + \nu \Delta \mathbf{u}, \quad (1.5.1)$$

$$\nabla \cdot \mathbf{u} = 0, \quad (1.5.2)$$

where the primes have been dropped for notational simplicity.

A canonical stability problem of long-standing interest is flow in a plane channel (Fig. 1.2), also referred to as plane Poiseuille flow, which is confined in the wall-normal (y) direction between infinite plates. This idealized laminar flow is driven by a constant pressure gradient in the streamwise (x) direction, and there are no boundaries in either the streamwise or spanwise (z) directions. The nondimensional mean flow is parallel and is given by

$$\mathbf{u}_0(\mathbf{x}) = (u_0(y), 0, 0)^T, \quad u_0(y) = 1 - y^2, \quad p_0(\mathbf{x}) = -\frac{2}{\text{Re}}x, \quad (1.5.3)$$

where distances have been scaled by the half-channel width h , velocities by the centerline velocity $u_c = u_0(0)$, and the Reynolds number Re is given by $\text{Re} = u_c h / \nu$. (Just as we dropped the primes for notational convenience, we also drop the “*”, heretofore used to denote nondimensional quantities.)

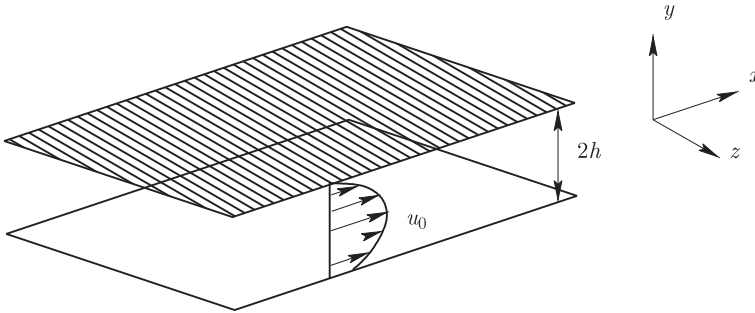


Fig. 1.2. Plane channel flow. The x , y and z directions are called the streamwise, normal and spanwise directions, respectively

The linear stability of this flow is assessed by studying perturbations of the form

$$\begin{aligned} \mathbf{u}(\mathbf{x}, t) &= Re \left\{ \hat{\mathbf{u}}(y) e^{i(\alpha x + \beta z) - i\omega t} \right\} , \\ p(\mathbf{x}, t) &= Re \left\{ \hat{p}(y) e^{i(\alpha x + \beta z) - i\omega t} \right\} , \end{aligned} \quad (1.5.4)$$

where α , β and ω are complex constants, and Re denotes the real part of a complex quantity. (Note the slight difference between the symbols for the Reynolds number (Re) and the real part (Re).) Equations (1.5.1) and (1.5.2) become, in component form,

$$\{\mathcal{D}^2 - (\alpha^2 + \beta^2) - i\alpha Re u_0\} \hat{u} - Re(\mathcal{D}u_0) \hat{v} - i\alpha Re \hat{p} = -i\omega Re \hat{u} , \quad (1.5.5)$$

$$\{\mathcal{D}^2 - (\alpha^2 + \beta^2) - i\alpha Re u_0\} \hat{v} - Re \mathcal{D} \hat{p} = -i\omega Re \hat{v} , \quad (1.5.6)$$

$$\{\mathcal{D}^2 - (\alpha^2 + \beta^2) - i\alpha Re u_0\} \hat{w} - i\beta Re \hat{p} = -i\omega Re \hat{w} , \quad (1.5.7)$$

$$i\alpha \hat{u} + \mathcal{D} \hat{v} + i\beta \hat{w} = 0 , \quad (1.5.8)$$

where $\mathcal{D} = d/dy$. The boundary conditions are

$$\hat{u} = \hat{v} = \hat{w} = 0 \quad \text{at } y = \pm 1 . \quad (1.5.9)$$

The system (1.5.5)–(1.5.9) describes a *dispersion relation* between α , β and ω with Re as a parameter. If four real quantities out of α , β and ω are prescribed, then the dispersion relation constitutes an eigenvalue problem for the remaining two real quantities. If α and β are fixed, real quantities, then ω is the complex eigenvalue. When approached in this manner, the problem is one of *temporal stability*. If $Im(\omega) > 0$, then the corresponding mode grows in time, and the mean flow will be disrupted. The equilibrium solution, then, is unstable if a growing mode exists for any real α and β . An alternative approach to this problem is one of *spatial stability*. Here, ω is real and fixed, and two relations are imposed upon α and β to complete the specification of the problem (Nayfeh (1980), Cebeci and Stewartson (1980)). If $Im(\alpha) > 0$ or $Im(\beta) > 0$, then the mode grows in space. If such growing modes exist for any real ω and for any orientations of the waves, then the flow is spatially unstable. Gaster (1962) has given a procedure for relating the results of temporal and spatial stability analyses. Huerre and Monkewitz (1990) provide a valuable discussion of the physical aspects of the spatial stability problem.

By manipulating (1.5.5)–(1.5.8) we arrive at

$$\begin{aligned} &[\mathcal{D}^2 - (\alpha^2 + \beta^2)]^2 \hat{v} - i\alpha Re u_0 [\mathcal{D}^2 - (\alpha^2 + \beta^2)] \hat{v} + i\alpha Re (\mathcal{D}^2 u_0) \hat{v} \\ &= -i\omega Re [\mathcal{D}^2 - (\alpha^2 + \beta^2)] \hat{v} \end{aligned} \quad (1.5.10)$$

and

$$\begin{aligned} & [\mathcal{D}^2 - (\alpha^2 + \beta^2)](\alpha\hat{w} - \beta\hat{u}) - i\alpha\text{Re } u_0(\alpha\hat{w} - \beta\hat{u}) \\ &= -i\omega\text{Re } (\alpha\hat{w} - \beta\hat{u}) - \beta\text{Re } (\mathcal{D}u_0)\hat{v} . \end{aligned} \quad (1.5.11)$$

The first of these is the celebrated *Orr–Sommerfeld equation*, and it is subjected to the boundary conditions

$$\hat{v} = \mathcal{D}\hat{v} = 0 \quad \text{at } y = \pm 1 . \quad (1.5.12)$$

(The condition on $\mathcal{D}\hat{v}$ follows from (1.5.8) and (1.5.9).) The quantity $\alpha\hat{w} - \beta\hat{u}$ is the normal component of the perturbation vorticity. It satisfies

$$\alpha\hat{w} - \beta\hat{u} = 0 \quad \text{at } y = \pm 1 . \quad (1.5.13)$$

For this reason (1.5.11) is often referred to as the *vertical vorticity equation* (although Herbert (1983b) called it the *Squire equation*). Hence, there are two distinct classes of solutions to the sixth-order system (1.5.5)–(1.5.9). The first class comprises the eigenmodes of (1.5.10) and (1.5.12), with (1.5.11) serving merely to determine the vertical vorticity of this mode. The second class has $\hat{v} \equiv 0$ and contains the eigenmodes of (1.5.11) and (1.5.13). Squire (1933) showed that all solutions of the second class are damped modes. Until the role of the vertical vorticity modes in the weakly nonlinear stage of transition was recognized in the 1980s (Herbert (1983b)), attention had been focused almost exclusively on the Orr–Sommerfeld solutions. Note that in the temporal stability problem the eigenvalue ω enters linearly, whereas in the spatial stability problem the eigenvalue α enters nonlinearly.

There are numerous other incompressible flows whose linear stability can be assessed by similar mathematical formulations, e.g., circular Poiseuille flow (pipe flow), Taylor–Couette flow (flow between rotating cylinders or rotating spheres), and free shear layers. Of course, the nondimensionalizations and coordinate systems may differ. Moreover, in many cases, e.g., Taylor–Couette flow, the set (1.5.5)–(1.5.8) of three second-order equations and one first-order equation cannot be reduced to the Orr–Sommerfeld and vertical-vorticity equations (1.5.12)–(1.5.13).

1.5.2 Compressible Linear Stability

The stability of compressible flows has not attracted nearly the amount of attention devoted to the stability of incompressible flows. Indeed, there has yet to appear a single text devoted to the subject, and it goes unmentioned in all but the most recent texts on hydrodynamic stability, such as Schmid and Henningson (2001) and Criminale, Jackson and Joslin (2003). The basic concepts and approach to the stability theory of compressible laminar boundary layers are similar to those of the incompressible counterpart. However,

there are some fundamental differences, which will be discussed here following a brief historical overview.

Although Kuchemann (1938) must be credited with the first attempt to develop a compressible stability theory (which neglected the viscosity and the mean temperature gradient and was thus too restrictive), it was Lees and Lin (1946) who laid the foundation of an asymptotic theory analogous to that for the incompressible case. This asymptotic theory was further developed by Dunn (1953) and Dunn and Lin (1955). Mack (1969) provided comprehensive viscous and inviscid instability results for the flat-plate boundary layer for Mach numbers up to 10.

The first major difference from the incompressible linear stability theory is that from a mathematical point of view, the eigenvalue problem of the incompressible parallel flow is governed by a sixth-order system of ordinary differential equations (sometimes reducible to a fourth-order equation and a second-order equation), whereas the linear stability of compressible parallel flow is governed by an eighth-order system of ordinary differential equations. A key result is that the normal derivative of the mass-weighted streamwise velocity gradient $(\rho u')'$, where the prime stands for $\mathcal{D} = d/dy$, plays the same critical role as the curvature of the streamwise velocity (proportional to u'') in the incompressible theory. Consequently, the compressible flat-plate boundary layer is unstable to purely inviscid disturbances in contrast to the incompressible case where the instability, called the Tollmien–Schlichting instability, is of viscous origin. In supersonic boundary layers, these disturbances (known as the first modes) are most amplified when oblique. Wall cooling stabilizes these disturbances, as it tends to eliminate the generalized inflection point (where $(\rho u')' = 0$) within the boundary layer.

A second major difference between the compressible and incompressible theories arises in those circumstances in which the mean flow is supersonic relative to the phase velocity of the disturbance. Whenever the relative flow is supersonic over some portion of the boundary-layer profile, there are an infinite number of wavenumbers for the single phase velocity (Mack 1969). Associated with each of these so-called neutral disturbances is a family of unstable disturbances. The first of these modes is called Mack’s second mode, and it is the dominant mode of instability in the hypersonic regime. This mode is destabilized by wall cooling, as that tends to increase the region of supersonic relative mean flow within the boundary layer.

Following Mack’s pioneering numerical work, Malik (1982, 1990) developed efficient, high-order computational techniques for the solution of compressible stability problems, and demonstrated the use of the theory for analyzing supersonic and hypersonic transition experiments (Malik 1989). The theory has been extended to include real gas effects and the second mode disturbances were found to be relevant in boundary-layer transition over re-entry vehicles (Malik 2003).

Flow past solid boundaries, such as the flat plate illustrated in Fig. 1.3, have been the subject of many compressible linear stability studies. The cus-

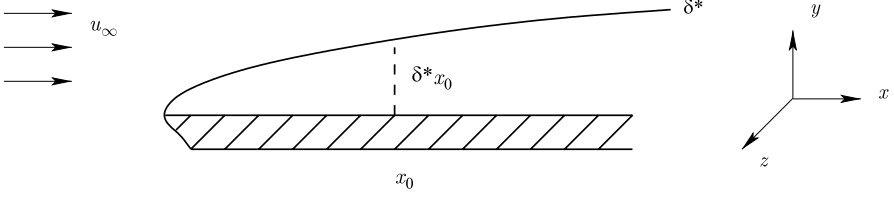


Fig. 1.3. Flow past a flat plate. The x , y and z directions are called the streamwise, normal and spanwise directions, respectively

tomary scaling for such flows is that distances are scaled by the boundary-layer displacement thickness δ^* (see (1.3.58)), while the velocity, density and temperature are scaled by their free-stream values at $y = \infty$, i.e., by u_∞ , ρ_∞ and T_∞ , respectively. We choose to scale the pressure by $p_\infty = \rho_\infty \mathcal{R} T_\infty$, where \mathcal{R} is the gas constant. (An alternative scaling for the pressure uses $\rho_\infty u_\infty^2$.) We assume that the gas is thermally perfect and that the ratio, λ/μ , of the second coefficient of viscosity to the first coefficient of viscosity and the Prandtl number Pr are also constants. The Reynolds number Re is defined by

$$\text{Re} = \rho_\infty U_\infty \delta^* / \mu_\infty , \quad (1.5.14)$$

and the free-stream Mach number M_∞ is given by

$$\text{M}_\infty = U_\infty / \sqrt{\gamma \mathcal{R} T_\infty} . \quad (1.5.15)$$

As indicated by the figure, the boundary-layer displacement thickness increases in the streamwise direction. The flow is certainly nonparallel within the boundary layer, and the velocity in the wall-normal (y) direction is nonzero. However, $|v_0| \ll u_0$, and the x dependence is much weaker than that on y . The simplest approach to boundary-layer stability analysis is to make the *parallel flow approximation*. Here, one analyzes the stability in the vicinity of some point x_0 by supposing that $u_0(x, y)$ is given by $u_0(x_0, y)$ for all x (likewise for the temperature and pressure) and that v_0 is negligible. This approximation is illustrated in Fig. 1.4. Within this approximation it is customary to take for the mean flow the solution to the boundary-layer equations. It is assumed that the variation of the mean flow over the streamwise wavelength $2\pi/\alpha$ of the perturbation is negligible. This approximation has proven to capture many, but not all, of the qualitative features of boundary-layer stability, and often provides acceptable quantitative results. See Sect. 1.6 for more sophisticated approaches.

As in the case of the incompressible linear stability equations, let the mean flow quantities be denoted by the subscript 0, and take perturbations in the same form as (1.5.4). The equation of state (1.2.15) becomes

$$\hat{p} = \frac{\hat{\rho}}{\rho_0} + \frac{\hat{T}}{T_0} . \quad (1.5.16)$$

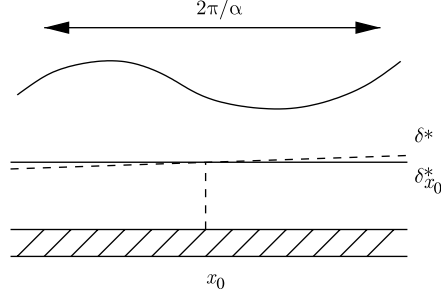


Fig. 1.4. The parallel boundary layer. The variation of the displacement thickness δ^* over one wave length $2\pi/\alpha$ of a perturbation is neglected

Following Malik and Orszag (1987), we use the disturbance variables in the combination

$$\hat{\mathbf{q}} = (\alpha\hat{u} + \beta\hat{w}, \hat{v}, \hat{p}, \hat{T}, \alpha\hat{w} - \beta\hat{u})^T. \quad (1.5.17)$$

(Note that \hat{T} denotes the temperature perturbations, whereas the superscript T denotes the transpose.) Furthermore, let

$$\begin{aligned} \zeta &= 2 + \frac{\lambda}{\mu}, & \mathcal{G} &= (\gamma - 1)M_\infty^2 \text{Pr}, & \mathcal{U}_0 &= \alpha u_0 + \beta w_0, \\ \mathcal{V}_0 &= \alpha w_0 - \beta u_0, & \varpi^2 &= \alpha^2 + \beta^2, & \varphi &= \mathcal{U}_0 - \omega. \end{aligned} \quad (1.5.18)$$

Starting from the continuity equation (1.3.11), the nonconservative form of the momentum equation (1.3.12) and the temperature equation (1.3.20), with the equation of state used to replace the density with the pressure, the compressible linear stability equations can be written as one first-order equation and four second-order equations:

$$A \mathcal{D}^2 \hat{\mathbf{q}} + B \mathcal{D} \hat{\mathbf{q}} + C \hat{\mathbf{q}} = \mathbf{0}, \quad (1.5.19)$$

subject to the boundary conditions that the velocity and temperature disturbances vanish at both boundaries:

$$\begin{aligned} \hat{v} &= 0 & \text{at } y = 0, \infty, \\ \alpha\hat{u} + \beta\hat{w} &= 0 & \text{at } y = 0, \infty, \\ \alpha\hat{w} - \beta\hat{u} &= 0 & \text{at } y = 0, \infty, \\ \hat{T} &= 0 & \text{at } y = 0, \infty. \end{aligned} \quad (1.5.20)$$

There is no boundary condition on the disturbance pressure. Even if the mean flow satisfies an adiabatic wall temperature boundary condition, i.e., $\mathcal{D}T_0 = 0$, the disturbance temperature is assumed to vanish at the wall on the grounds that the time scale for the disturbance is too short for it to achieve an adiabatic state.

The coefficient matrices in (1.5.19) are given by

$$A = \begin{pmatrix} 1 & 0 & 0 & 0 & 0 \\ 0 & 1 & 0 & 0 & 0 \\ 0 & 0 & 0 & 0 & 0 \\ 0 & 0 & 0 & 1 & 0 \\ 0 & 0 & 0 & 0 & 1 \end{pmatrix}, \quad (1.5.21)$$

$$B = \begin{pmatrix} \frac{1}{\mu_0} \frac{d\mu_0}{dT_0} T_0' & i(\zeta - 1)\varpi^2 & 0 & \frac{1}{\mu_0} \frac{d\mu_0}{dT_0} \mathcal{U}_0' & 0 \\ i \frac{\zeta - 1}{\zeta} & \frac{1}{\mu_0} \frac{d\mu_0}{dT_0} T_0' - \frac{\text{Re}}{\mu_0 \zeta} & 0 & 0 & 0 \\ 0 & 1 & 0 & 0 & 0 \\ \frac{2\mathcal{G}\mathcal{U}_0'}{\varpi^2} & 0 & 0 & \frac{2}{\mu_0} \frac{d\mu_0}{dT_0} T_0' & \frac{2\mathcal{G}\mathcal{V}_0'}{\varpi^2} \\ 0 & 0 & 0 & \frac{1}{\mu_0} \frac{d\mu_0}{dT_0} \mathcal{V}_0' & \frac{1}{\mu_0} \frac{d\mu_0}{dT_0} T_0' \end{pmatrix}, \quad (1.5.22)$$

and

$$C = \begin{pmatrix} -\frac{i\text{Re}}{\mu_0 T_0} \varphi - \zeta \varpi^2 & C_{12} & -\frac{i\text{Re}}{\mu_0} \varpi & C_{14} & 0 \\ i \frac{\zeta - 1}{\zeta \mu_0} \frac{d\mu_0}{dT_0} T_0' - \frac{i\text{Re}}{\mu_0 T_0 \zeta} \varphi - \frac{\varpi^2}{\zeta} & 0 & \frac{i}{\zeta \mu_0} \frac{d\mu_0}{dT_0} \mathcal{U}_0' & 0 & 0 \\ i & -\frac{T_0'}{T_0} & i\gamma M_\infty^2 \kappa & -\frac{i}{T_0} \varphi & 0 \\ 0 & C_{42} & \frac{i\text{Re}}{\mu_0} \mathcal{G} \varphi & C_{44} & 0 \\ 0 & -\frac{\text{Re}}{\mu_0 T_0} \mathcal{V}_0' & 0 & C_{54} & -\frac{i\text{Re}}{\mu_0 T_0} \kappa - \varpi^2 \end{pmatrix}, \quad (1.5.23)$$

where a prime on a mean flow variable denotes the wall-normal derivative of the quantity, e. g., $T_0' = \mathcal{D}T_0$. The remaining matrix elements are

$$\begin{aligned} C_{12} &= -\frac{\text{Re}}{\mu_0 T_0} \mathcal{U}_0' + \frac{i}{\mu_0} \frac{d\mu_0}{dT_0} T_0' \varpi^2, & C_{14} &= \mathcal{U}_0' \frac{1}{\mu_0} \frac{d^2 \mu_0}{dT_0^2} T_0' + \mathcal{U}_0'' \frac{1}{\mu_0} \frac{d\mu_0}{dT_0}, \\ C_{42} &= -\frac{\text{Re Pr}}{\mu_0 T_0} T_0' + 2i\mathcal{G}\mathcal{U}_0', \\ C_{44} &= -\frac{i\text{Re Pr}}{\mu_0 T_0} \varphi - \varpi^2 + \frac{\mathcal{G}}{\mu_0} \frac{d\mu_0}{dT_0} (U_0'^2 + W_0'^2) + \frac{1}{\mu_0} \frac{d^2 \mu_0}{dT_0^2} (T_0')^2 + \frac{1}{\mu_0} \frac{d\mu_0}{dT_0} T_0'', \\ C_{54} &= \frac{1}{\mu_0} \frac{d^2 \mu_0}{dT_0^2} T_0' \mathcal{V}_0' + \frac{1}{\mu_0} \frac{d\mu_0}{dT_0} \mathcal{V}_0''. \end{aligned} \quad (1.5.24)$$

This formulation allows reduction in order of the governing equations if viscous dissipation is neglected (i. e., $B_{25} = 0$), which has a small effect on the

unstable eigenvalue for small Mach numbers. Other forms of the compressible stability equations are given in Malik (1990).

1.6 Stability Equations for Nonparallel Flows

Only since the late 1970s have more sophisticated approaches than the parallel-flow assumption been employed for the study of the stability of nonparallel flows. These approaches include matched asymptotic expansions, triple-deck theory and parabolized equations. We shall focus here on the latter, as spectral methods have rarely been used in the context of the other approaches.

The parabolized stability equations (PSE) approach was developed for incompressible flow by Herbert (1991). Further details and developments can be found in Bertolotti (1991) and Bertolotti et al. (1992) for incompressible flows, and in Chang et al. (1991), Bertolotti and Herbert (1991) for compressible flow and Malik (2003) for hypersonic flow including chemistry effects. Schmid and Henningson (2001) furnish detailed derivations and equations for the incompressible case. Herbert (1997) reviews applications of PSE to both linear and nonlinear stability problems, for incompressible as well as compressible flows. The PSE permit the stability analysis of many mean flows that depend upon both the streamwise and wall-normal directions. These include flow past a flat plate (see Fig. 1.3), as well as flows of engineering interest such as flow past an airplane or a submarine.

The parabolized stability equations are developed by representing the total flow as a mean flow plus a disturbance field and decomposing the disturbance into a rapidly varying wave-like part and a slowly varying shape function. As a complete description of the PSE would take up several pages, we confine ourselves here to just providing an outline of the approach and illustrating the mathematical structure of the equations, using two-dimensional incompressible flow as the setting. Let $\mathbf{q} = (u, v, p)^T$ represent the disturbance field and write

$$\mathbf{q}(x, y, t) = \text{Re} \{ \hat{\mathbf{q}}(x, y) \chi(x, t) \} , \quad (1.6.1)$$

with

$$\chi(x, t) = \exp \left(i \int_{x_0}^x \alpha(\psi) \, d\psi - \omega t \right) , \quad (1.6.2)$$

where $\alpha(x)$ is a local complex wavenumber that captures the rapidly varying part, ω is the frequency, and $\hat{\mathbf{q}}$ is the slowly varying (in x) shape function. Constraints of the type

$$\int_0^\infty \left(\bar{\hat{u}} \frac{\partial \hat{u}}{\partial x} + \bar{\hat{v}} \frac{\partial \hat{v}}{\partial x} \right) dy = 0 , \quad (1.6.3)$$

where the overbar denotes the complex conjugate, impose a condition on $\alpha(x)$ such that most of the waviness and growth of the disturbance are absorbed into the exponential function χ in (1.6.2), making the shape function $\hat{\mathbf{q}}$ slowly varying with x . The ellipticity is retained for the wave part while parabolization is applied to the shape function. Hence, the $\hat{\mathbf{q}}_{xx}$ terms in the governing equations are dropped, and we arrive at a set of equations in which the only second-order derivatives are those with respect to y .

The linear parabolized stability equations are derived from the Navier–Stokes equations with the usual linearization procedure plus the parabolization approach discussed above. The linear PSE may be written as

$$\frac{\partial \hat{\mathbf{q}}}{\partial x} = L_0 \hat{\mathbf{q}} + L_1 \frac{\partial \hat{\mathbf{q}}}{\partial y} + L_2 \frac{\partial^2 \hat{\mathbf{q}}}{\partial y^2}. \quad (1.6.4)$$

The boundary conditions are

$$\hat{u} = 0, \quad \hat{v} = 0 \quad \text{at} \quad y = 0, \infty, \quad (1.6.5)$$

supplemented with appropriate inflow conditions at $x = x_0$.

The matrices in (1.6.4) are given by

$$L_0 = \begin{pmatrix} -i\alpha & 0 & 0 & 0 \\ 0 & -i\alpha + \frac{i\omega}{u_0} - \frac{\alpha^2}{u_0 \text{Re}} - \frac{1}{u_0} \frac{\partial v_0}{\partial y} & 0 & 0 \\ i\omega - \frac{\alpha^2}{\text{Re}} - \frac{\partial u_0}{\partial x} & -\frac{\partial u_0}{\partial y} & -i\alpha & 0 \end{pmatrix}, \quad (1.6.6)$$

$$L_1 = \begin{pmatrix} 0 & -1 & 0 \\ 0 & -\frac{v_0}{u_0} - \frac{1}{u_0} & 0 \\ -v_0 & u_0 & 0 \end{pmatrix}, \quad L_2 = \begin{pmatrix} 0 & 0 & 0 \\ 0 & \frac{1}{\text{Re} u_0} & 0 \\ \frac{1}{\text{Re}} & 0 & 0 \end{pmatrix}.$$

Note that α is a complex function of x , u_0 and v_0 are real functions of x and y , and Re and ω are real constants.

For the nonlinear PSE approximation, the disturbance function can be expressed by the following truncated Fourier series

$$\mathbf{q}(x, y, t) = \sum_{m=-M}^M \hat{\mathbf{q}}_m(x, y) \chi_m(x, t) + \text{complex conjugate}, \quad (1.6.7)$$

where

$$\chi_m(x, t) = \exp \left(i \int_{x_0}^x \alpha_m(\psi) d\psi - m\omega t \right). \quad (1.6.8)$$

Following a similar parabolization strategy, one obtains for each Fourier mode $\hat{\mathbf{q}}_m(x, y)$ an equation that is structurally the same as (1.6.4) with the addition of a forcing term that accounts for the nonlinear interactions.

For further details, see Bertolotti, Herbert and Spalart (1992) for the full, nonlinear PSE description of incompressible flow, and see Chang et al. (1991) and Bertolotti and Herbert (1991) for the compressible formulation.

Finally, we conclude this survey with some brief remarks on triple deck theory. One line of approach has employed triple deck theory, (e.g., Smith (1979) and Hall (1983)), to derive a set of equations based on formal asymptotic expansions to account consistently for the spatial evolution of the mean flow and the instability. As the triple deck approaches have invariably employed finite-difference methods, we shall not discuss them further. (There appears to be no fundamental obstacle to the use of spectral methods for the triple deck approach.)

Spectral Methods

Evolution to Complex Geometries and Applications to
Fluid Dynamics

Canuto, C.; Hussaini, M.Y.; Quarteroni, A.; Zang, Th.A.

2007, XXX, 596 p., Hardcover

ISBN: 978-3-540-30727-3